

Electrogenerated Chemiluminescence. 81. Influence of Donor and Acceptor Substituents on the ECL of a Spirobifluorene-Bridged Bipolar System

Fernando Fungo,^{†,‡} Ken-Tsung Wong,[§] Sung-Yu Ku,[§] Ying-Yueh Hung,[§] and Allen J. Bard^{*,†}

Department of Chemistry and Biochemistry, The University of Texas at Austin, Austin, Texas 78712, and Department of Chemistry, National Taiwan University, 106 Taipei, Taiwan

Received: September 30, 2004; In Final Form: January 3, 2005

The electrochemistry and radical ion annihilation electrogenerated chemiluminescence (ECL) of 9,9'-spirobifluorene-bridged bipolar systems containing 1,3,4-oxadiazole-conjugated oligoaryl and triarylamine substituents were investigated. The stability of the oxidized spirobifluorenes was improved by functionalization with triarylamine centers. These donor–acceptor (DA) compounds exhibited a good fluorescence efficiency with an emission maximum that correlated with the potential difference between radical anion and cation formation, suggesting a charge transfer (CT) emission band. An ECL mechanism based on the formation of the CT excited state by radical ion annihilation or production of the triplet state followed by triplet–triplet annihilation, with perhaps some excimer contribution, is proposed.

Introduction

We describe here the electrochemical reduction and oxidation and radical ion annihilation electrogenerated chemiluminescence (ECL) of spirobifluorene compounds modified with acceptor and donor groups (Figure 1) in aprotic solution. The fluorene ring absorbs strongly in the UV region, fluoresces in the visible region, and shows good chemical and photochemical stability. Fluorene polymers have been extensively studied as electron transport materials^{1,2} and have also found applications as nonlinear optic materials^{3–5} and photovoltaic cells.^{6,7} Fluorene-based materials are usually highly fluorescent and are among the most promising candidates as light-emitting materials.^{1,2,8} The electrochemistry and ECL of fluorene derivatives and polyfluorene have been considered in previous studies.^{9–11} This work extends those results to novel compounds with more stable radical ions.

The ECL generation mechanism in solution is well-known.¹² The general scheme involves the alternate electrochemical production of radical cations and radical anions capable of undergoing energetic electron-transfer reactions. The subsequent annihilation reaction between the two ions generates excited states that lead to emission. Usually, there are three schemes for excited state production. The emitting state is a singlet state formed directly upon electron transfer (S-route) or by a triplet–triplet up-conversion reaction involving an intermediate triplet excited state formed in the electron-transfer reaction (T-route). In some cases, excimer or exciplex emission has also been observed (E-route).¹² Many polyaromatic hydrocarbons, the first compounds studied for ECL applications, produce emission by this reaction scheme.^{12–13} Useful ECL compounds must be able to generate stable radical cations and anions with sufficient energy in the electron transfer reaction to generate an excited state that emits with good quantum efficiency. However, many

good emitting molecules do not have these characteristics. In some cases, one of the redox processes is chemically irreversible because of decomposition of the radical ion. In others, the radical cation or anion cannot be generated before the background oxidation or reduction of the solvent-supporting electrolyte. In these cases, ECL coreactants must be added to generate a stable radical counterion required for annihilation.¹² ECL coreactants are species that, upon electrochemical oxidation or reduction, produce intermediates that react with other compounds to produce excited states capable of emitting light.^{12,14}

In recent years, compounds that contain the coreactant directly attached to the emitting dye with one reversible electrochemical process, or compounds that have donor and acceptor moieties covalently bonded with a capability to generate ECL through charge-transfer states, have been studied^{15,16} with the hope of improving the radical cation and anion stability and obtaining structures that contain charge transfer (CT) characteristics analogous to those of Ru(bpy)₃²⁺.

The fluorene ring is a good emitting center but has poor cation radical stability so it is not a good candidate for ECL. However, by functionalization with the appropriate redox center, it is possible to improve the stability of the oxidized fluorene for ECL. Recently, the synthesis and photophysical properties of 9,9'-spirobifluorene-bridged bipolar systems containing 1,3,4-oxadiazole-conjugated oligoaryl and triarylamine moieties have been reported (Figure 1).¹⁷ The notation used for these is **D_mA_n**, where *m* indicates the number of donor (diphenylamine) groups and *n* is the number of acceptor (oxadiazole) groups. These compounds exhibit an efficient photoinduced excitation characteristic of a CT emission band. In the present study, we investigated electrochemical, photophysical, and ECL properties of these new donor–acceptor spirobifluorene derivatives aimed at correlating their electrochemical properties and ECL behavior.

Experimental Procedures

Materials. Anhydrous benzene and anhydrous acetonitrile (Aldrich) were used as received. Tetra-*n*-butylammonium perchlorate (TBAP) (Aldrich) was dried in a vacuum oven at 125

* Corresponding author. Phone: (512) 471-3761. Fax: (512) 471-0088. E-mail: ajbard@mail.utexas.edu.

[†] The University of Texas at Austin.

[‡] Current address: Departamento de Química, Universidad Nacional de Río Cuarto, Agencia Postal 3 (5800), Río Cuarto, Argentina.

[§] National Taiwan University.

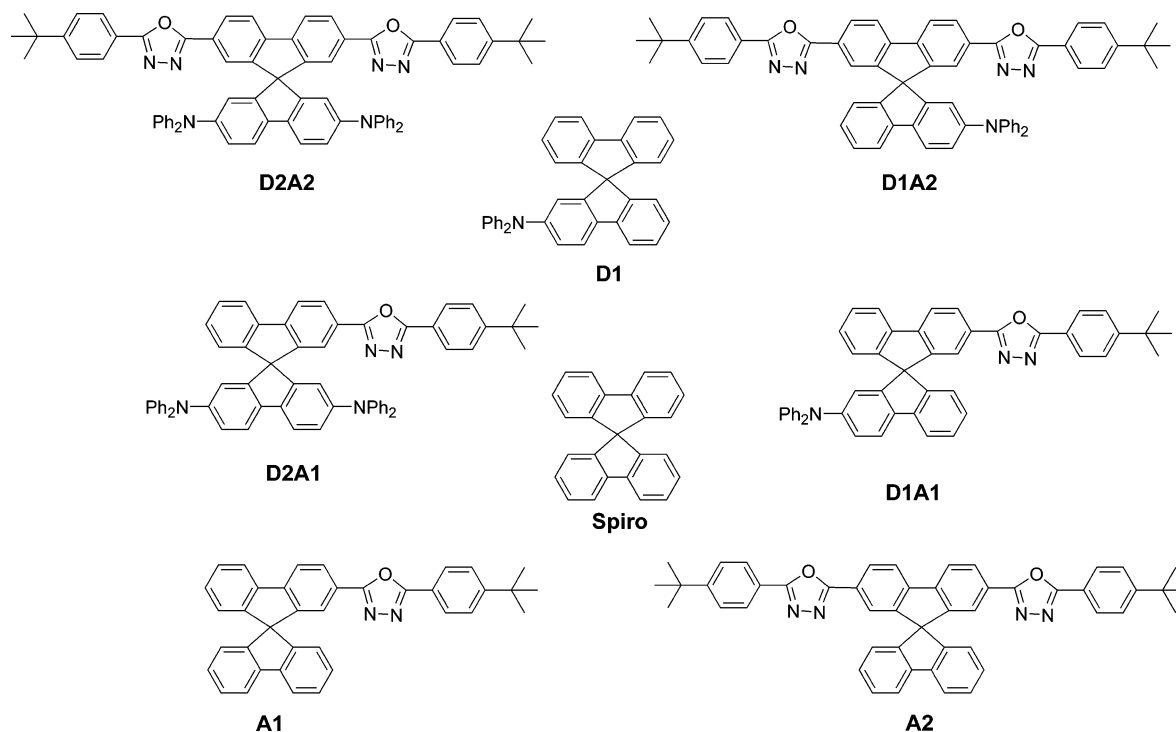


Figure 1. DA molecular structures.

°C prior to being transferred directly into an inert atmosphere drybox (Vacuum Atmospheres Corp., Hawthorne, CA). All solutions were prepared in the drybox with fresh anhydrous solvents and sealed in airtight vessels for measurements completed outside the drybox.

The synthesis and characterization of the spirobifluorene compounds have been described elsewhere.¹⁷ Ru(bpy)₃(ClO₄)₂ was obtained by commercially available Ru(bpy)₃Cl₂ (Aldrich) being converted by a metathesis reaction with an excess of NaClO₄ (Fluka) and then recrystallizing twice from an ethanol–acetone (5:1) solution.^{18,19}

Characterizations. Cyclic voltammograms were recorded on a CH Instruments Electrochemical Work Station (Austin, TX). The working electrode in all cases consisted of an inlaid platinum disk (2.0 mm diameter) that was polished on a felt pad with 0.3 μm alumina (Buehler, Ltd., Lake Bluff, IL), sonicated in water and absolute ethanol for 3 min, and then dried in an oven at 50 °C before being transferred into the inert atmosphere drybox. A platinum coil served as a counter electrode, and silver wire was utilized as a quasi reference electrode. The electrolyte consisted of a benzene–acetonitrile (4:1) solution with 0.1 M TBAP. Potential values were expressed relative to the potential for the oxidation of ferrocene (Fc), which was added to the electrolyte as an internal standard. ECL measurements were performed as previously reported.¹⁸ To generate the annihilation reaction, the working electrode was pulsed between the first oxidation and reduction peak potentials of the spirobifluorene compounds with a pulse width of 0.1 s. The resulting emission spectra were obtained with a charged coupled device (CCD) camera (Photometrics CH260, Photometrics-Roper Scientific, Tucson, AZ) that was cooled to –100 °C. Integration times were 2 min. The CCD camera and grating system were calibrated with a mercury lamp prior to each measurement. Absorption spectra were obtained in a Hewlett-Packard array spectrophotometer Model 8453, and the steady-state fluorescence spectra were recorded at room temperature using a PTI spectrofluorimeter (Model QM-2000; Photon Technology International, Lawrenceville, NJ).

Results and Discussion

Electrochemistry. Cyclic voltammetry (CV) was used to obtain information about the energetics for formation and stability of the species DA^{•-}, DA²⁻, DA^{•+}, and DA²⁺. The electrochemistry and ECL behavior were studied in benzene/MeCN (4:1) containing 0.1 M TBAP as a supporting electrolyte because of the low solubility of these compounds in polar solvents such as MeCN; this solvent system has a sufficiently wide electrochemical window to detect the redox processes of interest. Typical CVs obtained are shown in Figure 2. **D2A2** and **D2A1** are unusual in that they show two chemically reversible waves for both oxidation and reduction. All peak currents (*i_p*) observed correspond to one electron process, and scan rate (*v*) studies showed that all of the reduction and oxidation current peaks were proportional to the square root of *v* indicating diffusion governed electrochemical processes. Table 1 contains a summary of the electrochemical data.

Oxidation Behavior. The number of oxidation waves in the DA molecules depended on the number of the diphenylamine substituents. The **D2A1** and **D2A2** first oxidation peak potential was 200 mV less positive than that of **D1A1** and **D1A2**, showing that the addition of a second diphenylamine group to the fluorene ring makes the molecule much easier to oxidize. This indicates that the radical cation is stabilized by charge delocalization through the fluorene ring. The removal of a second electron from positively charged **D2A1** and **D2A2** centers is more difficult than the first oxidation process, producing two separate CV waves (Figure 2). On the other hand, the spirobifluorene moiety without this substituent and **A1** (Figure 1) showed only an irreversible oxidation process, with a peak potential at ~1.2 V versus Fc/Fc⁺, which can be assigned to the fluorene ring oxidation.²⁰ This shift in potential for oxidation is consistent with other aromatic species with amine substituents.

Reduction Behavior. The first reduction process in all of the compounds and the second reduction for **D1A2** and **D2A2** were reversible even at a low scan rate (~0.02 V/s), while in the case of **D1A1** and **D2A1**, the second processes were less

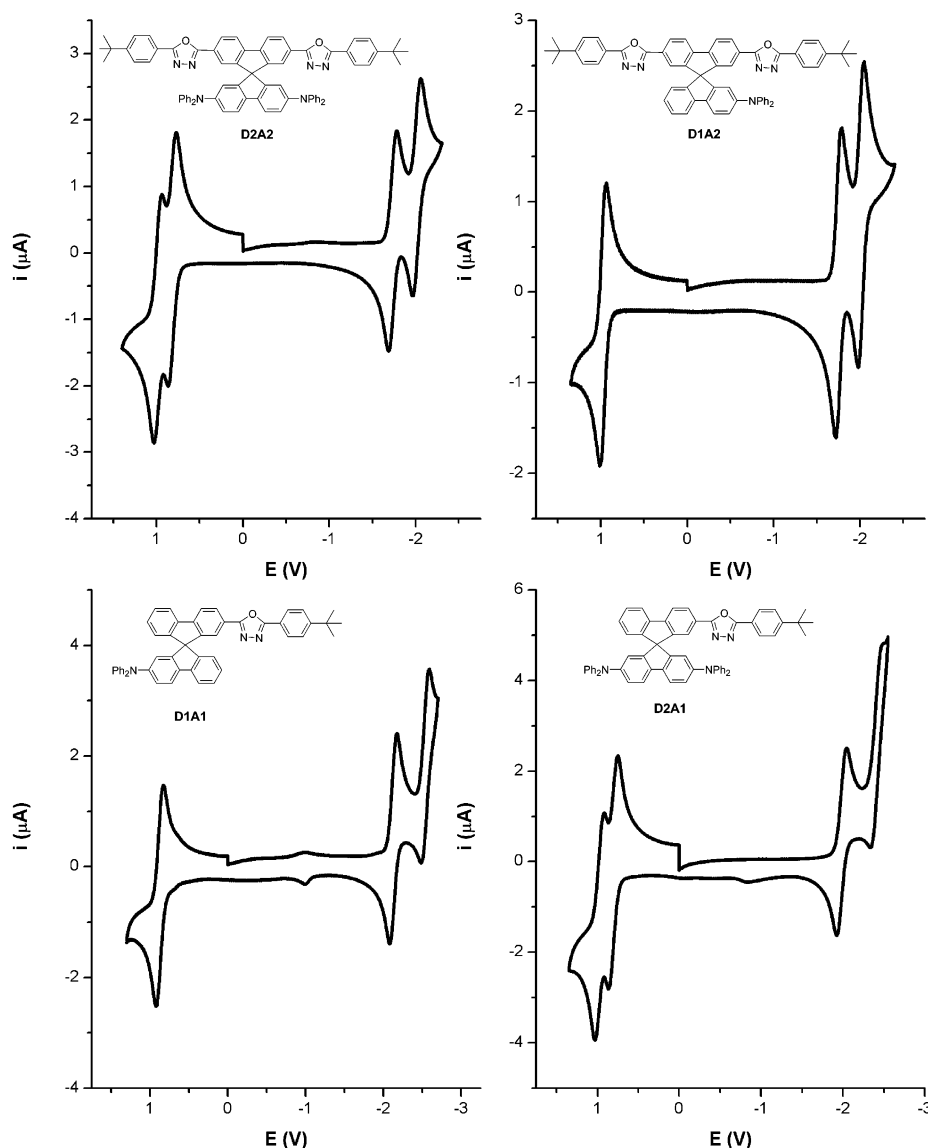


Figure 2. Cyclic voltammograms of **D2A2**, **D2A1**, and **D1A2** in PhH/MeCN (4:1) containing 0.1 M TBAP as supporting electrolyte. Scan rate 0.2 V/s. The electrode potential (E) is expressed vs a silver wire quasi-reference electrode.

TABLE 1: Electrochemical Properties^a

compounds	Red ₁ (V) ^b	Red ₂ (V) ^b	Red ₁ – Red ₂	Ox ₁ (V) ^b	Ox ₂ (V) ^b	Ox ₁ – Ox ₂	ΔE (V) ^c
Spiro	-3.19			$\sim 1.2^d$			
D1	-3.15			0.5			3.65
A1	-2.51	-2.90		$\sim 1.3^d$			
A2	-2.22	-2.49	0.27	$\sim 1.3^d$			
D1A1	-2.48	-2.92	0.42	0.5			2.98
D1A2	-2.22	-2.49	0.27	0.49			2.71
D2A1	-2.45	-2.88	0.43	0.28	0.46	0.18	2.73
D2A2	-2.25	-2.52	0.27	0.30	0.46	0.16	2.55

^a The potential value was expressed relative to the potential for the oxidation of ferrocene, which was added to the electrolyte as an internal standard. ^b Half-wave potentials. ^c $\Delta E = \text{Ox}_1 - \text{Red}_1$. ^d Irreversible electrochemical process.

reversible and became irreversible at scan rates below 0.2 V/s. The electrochemical data, summarized in Table 1, reflects the strong electron-accepting nature of the oxadiazole substituent. The **D1A2** and **D2A2** first reduction peak potential is 250 mV less negative than that in **D1A1** and **D2A1**, indicating the combined influence of the two substituent groups. The difference between the second reduction processes is more sensitive to the presence of a second oxadiazole group. The **D1A2** and **D2A2** second reduction peak potentials were ~ 430 mV less negative as compared to the second waves in **D2A1** and **D1A1**.

The reduction mechanism for the DA systems can be interpreted as follows. The first reduction process leads to the formation of the radical anion and the second to the corresponding dianion. The major portion of the electron density in the anionic species probably largely resides on the oxadiazole rings due to their electron-withdrawing (acceptor) character. The addition of the second electron is more difficult than the first because of Coulombic repulsion. For the molecules with two oxadiazole substituents, **D1A2** and **D2A2**, the two negative charges remain mostly in the oxadiazoles as opposed to **D1A1**

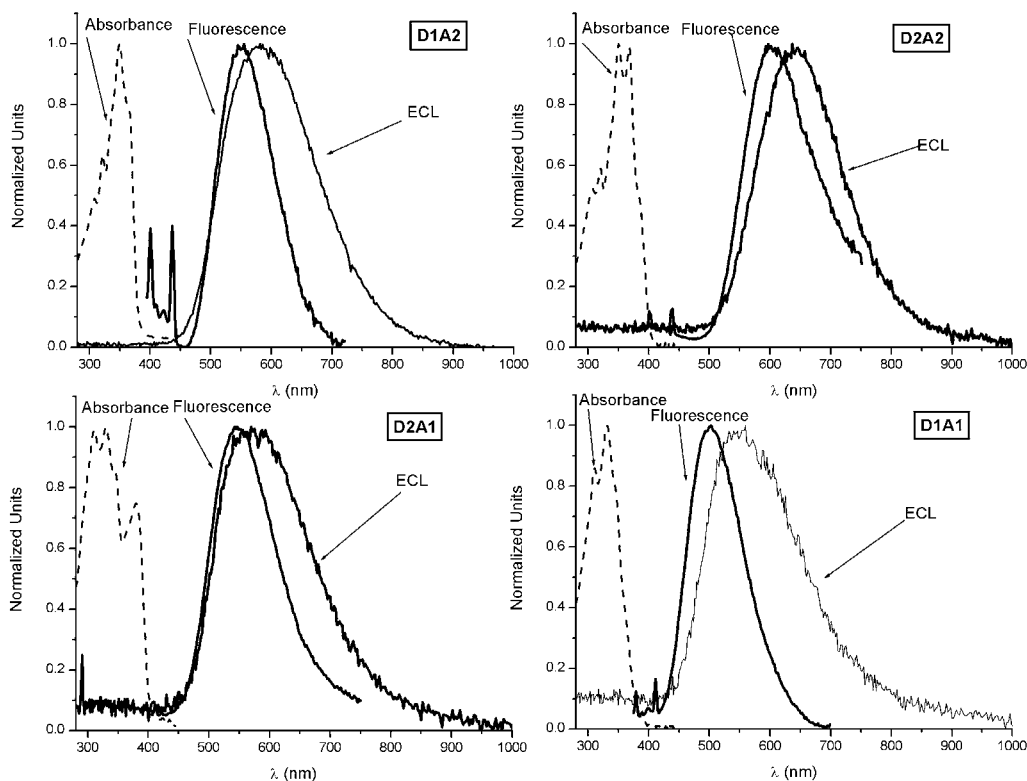


Figure 3. Absorbance, fluorescence, and ECL spectra of DA derivatives system in PhH/MeCN (4:1).

and **D2A1**, where more of the electron density resides in the fluorene ring. Moreover, in **D1A1** and **D2A1**, the fluorene reduction occurs at a less negative potential than in the unsubstituted compounds (compare these to the Spiro and D1 reduction potentials in Table 1). The greater delocalization causes the first reductions to be at lower potentials, but the better localization in the anionic radical on the oxadiazole ring renders the second reduction potentials to be much closer to the first reduction potentials for **D1A2** and **D2A2**.

Note that in the molecules under consideration here, the two fluorene rings are bonded perpendicularly through a common carbon bond. The A substituents are on one fluorene ring and the D substituents are on the other (Figure 1). Since the geometry impedes π orbital interactions between the two rings, inductive effects between the rings are minimal, and the redox potentials are only slightly affected by the substituents in a neighboring fluorene ring. Thus, the oxidation in **D1A1** occurs at about the same potential for **D1A2** and that in **D2A1** at about the same potential as **D2A2**.

Spectroscopy. The electronic absorption and emission spectra of **D1A1**, **D1A2**, **D2A1**, and **D2A2** were obtained in the same solvent mixture as used for the electrochemical measurements and are shown in Figure 3. The absorption maxima of these compounds are in the UV region; the energies of the zero-zero transition (E_{00}) are summarized in Table 2 and are assigned to the energy of the singlet state.¹⁷ In general, the absorption spectra exhibit a composite characteristic of the acceptor and donor spirobifluore parent compounds,¹⁷ with negligible interactions among the substituents in the ground state. In contrast, the incorporation of acceptor and donor groups in the spirobifluore system promotes strong interactions in the excited state. The emission spectra exhibited bands in the visible region considerably red-shifted from the absorption bands; their maxima are summarized in Table 2. The DA compounds show emission bands between 500 and 600 nm that are not seen in the **A1** or **D1** compound emission spectra (Table 2). The spectra suggest

TABLE 2: Spectroscopic and ECL Properties

compounds	λ_{em}^a nm (eV)	S_1 (eV) ^b	λ_{ECL} nm (eV)	ϕ_{ECL} (%)
Spiro	322 (3.85)	3.97		
D1	397 (3.12)	3.35		
A1	351 (3.53)	3.6		
A2	4.02 (3.08)	3.27		
D1A1	500 (2.48)	3.54	540 (2.3)	0.011
D1A2	550 (2.25)	3.25	580 (2.14)	0.021
D2A1	546 (2.27)	3.10	570 (2.17)	0.021
D2A2	600 (2.06)	3.16	635 (1.95)	0.26

^a From photoluminescence. ^b From absorbance.

excitation causes an intramolecular electron transfer, and the emission involves a CT process. This mechanism is supported by the strong solvent dependence of the spectral properties.¹⁷ Moreover, the CT emission maxima directly correlate with the energy of the charge separated state ($A^{\cdot-}D^{\cdot+}$), which can be estimated from the first DA oxidation and reduction potentials determined from the CV measurements (ΔE , Table 1). Figure 4 shows a good linear relationship between wavelength emission maxima and ΔE for the different DA systems, supporting the proposed CT emission mechanism.

ECL in Solution. All four DA spirobifluore derivatives produce ECL in PhH/MeCN (4:1) as shown in Figure 3. ECL was generated by applying repeated pulsing (pulse width, 0.1 s) between potentials of the first CV oxidation and reduction waves, where the radical cation and anion forms of the DA compounds are produced alternately. The ECL signals are about 40 nm to lower energies. This shift cannot be attributed to self-absorption because of the low absorbance of the DA compounds at the emitting wavelength (Figure 3).

The enthalpy available in the radical cation/radical anion annihilation reaction is given (in eV) by²¹

$$\Delta H_{ann}^0 = \Delta G^0 - T\Delta S^0 \approx \Delta E - 0.1 \text{ eV}$$

ΔG^0 can be obtained from the difference between the standard

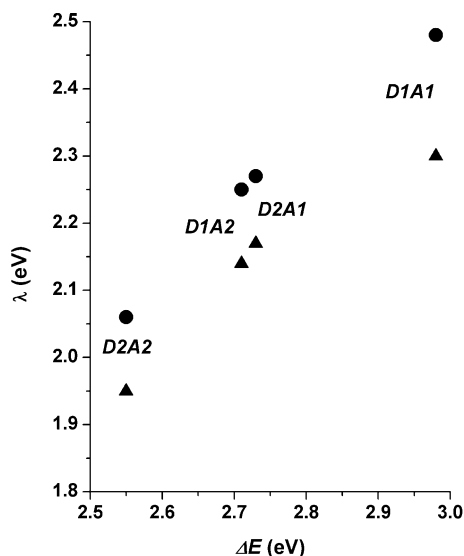


Figure 4. Plot between the photoemission (circles) and ECL (triangles) maxima wavelength vs the potential differences of the first oxidation and the first reduction waves.

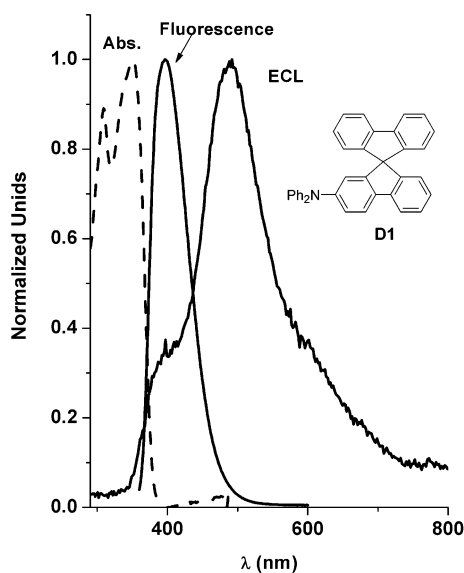


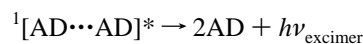
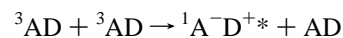
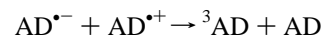
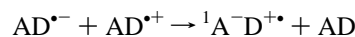
Figure 5. Absorbance, fluorescence, and ECL spectra of D1 molecule in PhH/MeCN (4:1).

potentials of the first oxidation and first reduction waves in the cyclic voltammogram (ΔE). For ECL, via the S-route, the following condition must be satisfied: $-\Delta H_{\text{ann}}^0 > E_s$, where E_s is the energy for the first excited singlet state, as estimated from both absorbance and photoluminescence spectra.²² In our case, we cannot observe the luminescence spectrum of the singlet state because before the emission, the charge transfer state is formed. As a consequence, we estimate the energy of singlet state from the first vibronic peak of the UV spectrum.¹⁷

The results in Tables 1 and 2 indicate that the four DA spirobifluorenes do not have enough energy supplied by the ion-annihilation reaction for direct production of the fluorene singlet state. They show the same kind of dependence of emission maxima with the energy of the charge-separated state as the DA fluorescence maxima (Figure 4). On the basis of the photophysical characteristics of the DA systems and the energy analysis, we propose that the ECL mechanism involves formation of a CT excited state. The energy supplied by the ion-annihilation reaction is enough for direct production of the emissive singlet CT state ($^1A^-D^{+*}$) or to form the excited triplet

(see ΔE in Table 1 and λ_{em} in Table 2). On the other hand, a triplet-triplet annihilation to form the singlet CT state is also a possibility. Note that the **D1** molecule does not show CT emission due to the absence of oxadiazole substituent. However, the presence of diphenylamine groups improves the oxidation stability. Tables 1 and 2 show that the energy supplied by the ion-annihilation reaction is enough for direct production of the emissive fluorene singlet state. The **D1** ECL spectrum shows a shoulder at 395 nm and a peak at 492 nm (Figure 5). The **D1** ECL emission energy is higher than those of the DAs. Therefore, the shoulder could be assigned to emission of the fluorene singlet and the peak to fluorene excimer. The **D1** ECL spectrum is similar to that obtained earlier for spirobifluorene systems without acceptor-donor moieties⁹ and supports the formation of a CT excited state in DA ECL.

The greater breadth of the ECL wave and the shift to longer wavelengths suggests that radical ion and TTA annihilation lead to some excimer formation, although the larger slit width needed to measure the fairly weak ECL emission probably also contributes. The following mechanism is consistent with these results.



Similar results were reported for the ECL of other fluorene derivatives and polyfluorene, where even large steric effects that should discourage excimer formation were found.^{9,10,19}

The relative ECL efficiencies of the DA compounds were determined by the number of photons emitted per injected electron being compared with the known $\text{Ru}(\text{bpy})_3^{2+}$ ECL efficiency,²³ and the results are listed in Table 2. The values obtained are relatively small as compared to those observed in other organic acceptor-donor ECL dyes and fluorene compounds.¹⁵

Conclusion

The functionalization of spirobifluorene with the appropriate electron acceptor and donor centers improved the stability of the radical ions and allowed the generation of ECL via annihilation reactions. The ECL and fluorescence emission maxima linearly correlated with the potential difference of the first oxidation and first reduction wave, suggesting the emission is from a CT state. This energy was less than that of the emitting state, so a triplet-triplet annihilation mechanism is suggested.

Acknowledgment. We thank the National Science Foundation (CHE 0109587) and the Consejo Nacional de Investigaciones Científicas y Técnicas (CONICET-Argentina) and Fundación Antorchas for their support. Financial support (NSC 93-2113-M-002-009) from the National Science Council of Taiwan is also acknowledged.

References and Notes

- (1) Mueller, C. D.; Falcou, A.; Reckefuss, N.; Rojahn, M.; Wiederhirn, V.; Rudati, P.; Frohne, H.; Nuyken, O.; Becker, H.; Meerholz, K. *Nature* **2003**, *421*, 829.

- (2) Culligan, S. W.; Geng, Y.; Chen, S. H.; Klubek, K.; Vaeth, K. M.; Tang, C. W. *Adv. Mater.* **2003**, *15*, 1176.
- (3) Epshtein, O.; Eichen, Y.; Ehrenfreund, E.; Wohlgenannt, M.; Vardeny, Z. V. *Phys. Rev. Lett.* **2003**, *90*, 046804/1.
- (4) Zhan, X.; Liu, Y.; Zhu, D.; Liu, X.; Xu, G.; Ye, P. *Chem. Phys. Lett.* **2002**, *362*, 165.
- (5) Zhan, X.; Liu, Y.; Zhu, D.; Huang, W.; Gong, Q. *Chem. Mater.* **2001**, *13*, 1540.
- (6) Cabanillas-Gonzalez, J.; Yeates, S.; Bradley, D. D. C. *Synth. Met.* **2003**, *139*, 637.
- (7) Pacios, R.; Bradley, D. D. C. *Synth. Met.* **2002**, *127*, 261.
- (8) (a) Pei, Q.; Yang, Y. *J. Am. Chem. Soc.* **1996**, *118*, 7416. (b) Becker, S.; Ego, C.; Grimsdale, A. C.; List, E. J. W.; Marsitzky, D.; Pogantsch, A.; Setayesh, S.; Leising, G.; Müllen, K. *Synth. Met.* **2002**, *125*, 73.
- (9) Choi, J. P.; Wong, K. T.; Chen, Y. M.; Yu, J. K.; Chou, P. T.; Bard, A. J. *J. Phys. Chem. B* **2003**, *107*, 14407.
- (10) Prieto, I.; Teetsov, J.; Fox, M. A.; Vanden Bout, D. A.; Bard, A. J. *J. Phys. Chem. A* **2001**, *105*, 520.
- (11) Kulkarni, A. P.; Kong, X.; Jenekhe, S. A. *J. Phys. Chem. B* **2004**, *108*, 8689.
- (12) Faulkner, L. R.; Bard, A. J. *Electroanalytical Chemistry*; Marcel Dekker: New York, 1977; Vol. 10, p 1. (b) Bard, A. J.; Debad, J. D.; Leland, J. K.; Sigal, G. B.; Wilbur, J. L.; Wohlstadter, J. N. *Encyclopedia of Analytical Chemistry: Applications, Theory, and Instrumentation*; Meyers, R. A., Ed.; John Wiley & Sons: New York, 2000; Vol. 11, p 9842 and references therein. (c) *Electrogenerated Chemiluminescence*; Bard, A. J., Ed.; Marcel Dekker: New York, 2004.
- (13) (a) Knight, A. W.; Greenway, G. M. *Analyst* **1994**, *119*, 879. (b) Maloy, J. T.; Bard, A. J. *J. Am. Chem. Soc.* **1971**, *93*, 5968. (c) Bezman, R.; Faulkner, L. R. *J. Am. Chem. Soc.* **1972**, *94*, 6324. (d) Debad, J. D.; Morris, J. C.; Lynch, V.; Magnus, P.; Bard, A. J. *J. Am. Chem. Soc.* **1996**, *118*, 2374. (e) Debad, J. D.; Morris, J. C.; Magnus, P.; Bard, A. J. *J. Org. Chem.* **1997**, *62*, 530.
- (14) (a) Chang, M.-M.; Saji, T.; Bard, A. J. *J. Am. Chem. Soc.* **1977**, *99*, 5399; (b) Rubinstein, I.; Bard, A. J. *J. Am. Chem. Soc.* **1981**, *103*, 512; (c) White, H. S.; Bard, A. J. *J. Am. Chem. Soc.* **1982**, *104*, 6891.
- (15) (a) Kapturkiewicz, A.; Grabowski, Z.; Jasny, J. *J. Electroanal. Chem.* **1990**, *279*, 55. (b) Kapturkiewicz, A. *Chem. Phys.* **1992**, *166*, 259. (c) Kapturkiewicz, A.; Herbich, J.; Nowacki, J. *Chem. Phys. Lett.* **1997**, *275*, 355.
- (16) (a) Lai, R. Y.; Kong, X.; Jenekhe, S. A.; Bard, A. J. *J. Am. Chem. Soc.* **2003**, *125*, 12631. (b) Lai, R. Y.; Fabrizio, E. F.; Lu, L.; Jenekhe, S. A.; Bard, A. J. *J. Am. Chem. Soc.* **2001**, *123*, 9112.
- (17) Chien, Y.-Y.; Wong, K.-T.; Chou, P.-T.; Cheng, Y.-M. *Chem. Commun.* **2002**, *23*, 2874.
- (18) McCord, P.; Bard, A. J. *J. Electroanal. Chem. Interfacial Electrochem.* **1991**, *318*, 91.
- (19) Gao, F. G.; Bard, A. J. *Chem. Mater.* **2002**, *14*, 3465.
- (20) Rault-Berthelot, J.; Granger, M. M.; Mattiello, L. *Synth. Met.* **1998**, *97*, 211.
- (21) Faulkner, L. R.; Bard, A. J. *Electroanalytical Chemistry*; Bard, A. J., Ed.; Marcel Dekker: New York, 1977; Vol. 10, pp 1–95.
- (22) Marcus R. A. *J. Phys. Chem.* **1989**, *93*, 3078.
- (23) Wallace, W. L.; Bard, A. J. *J. Phys. Chem.* **1979**, *83*, 1350.